Wavelength Dependence of Laser-Induced Damage: Determining the Damage Initiation Mechanisms

C. W. Carr,[1,2] H. B. Radousky,[1,2] and S. G. Demos[1]

[1]*Lawrence Livermore National Laboratory, 7000 East Avenue, Livermore, California 94551, USA*
[2]*University of California, Davis Physics Department, 1 Shields Avenue, Davis, California 95616, USA*

(Received 19 December 2002; published 19 September 2003)

A novel experimental approach is employed to understand the mechanisms of laser induced damage. Using an OPO (optical parametric oscillator) laser, we have measured the damage thresholds of deuterated potassium dihydrogen phosphate (DKDP) from the near ultraviolet into the visible. Distinct steps, whose width is of the order of k_BT, are observed in the damage threshold at photon energies associated with the number of photons ($3 \rightarrow 2$ or $4 \rightarrow 3$) needed to promote a ground state electron across the energy gap. The wavelength dependence of the damage threshold suggests that a primary mechanism for damage initiation in DKDP is a multiphoton process in which the order is reduced through excited defect state absorption.

DOI: 10.1103/PhysRevLett.91.127402 PACS numbers: 78.40.–q, 61.80.Ba

Potassium dihydrogen phosphate (KDP) is a remarkable material due to the combination of nonlinear optical and electro-optical properties and the speed (as fast as 20 mm/day) at which large (300 kg in weight) single crystals can be grown [1,2]. This unique combination of properties makes KDP technologically important and ideal for use as Pockel's cells, frequency doublers, and triplers on large aperture laser systems such as the National Ignition Facility and the Laser Megajoule [1]. It is also an ideal model system in which to study the role of intrinsic defects in complex oxide insulators.

Understanding the susceptibility of this class of perovskite materials in specific, and optical materials in general, to laser induced damage at laser fluences that are an order of magnitude below the expected intrinsic breakdown limits is a long-standing issue [3]. Several models proposed to explain this phenomenon include black or gray particles embedded in the optical material, lattice defects such as interstitial inclusions and vacancies, impact ionization by hot electrons (or electrons from shallow states), and multiphoton ionization [4–7]. Each of these models predicts a specific wavelength dependence of the damage threshold.

Throughout the literature, many different values have been quoted for the bulk laser induced damage threshold of KDP and its deuterated analog DKDP [8,9]. The spread in the data is not surprising considering that laser induced damage thresholds in optical materials depend on the duration of the laser pulse, focal spot geometry, variations between samples, previous exposure of the sample to laser radiation, and experimental technique [3,10–13]. These issues, when not addressed, can lead to a variation in experimental results of nearly 2 orders of magnitude. Consequently, this has made impossible a quantitative study of the wavelength dependent damage threshold by compiling work from many authors [8,9]. This issue is addressed in this work by making the first comprehensive multiwavelength damage threshold measurement in an optical material, namely, in DKDP. We have established that the previously mentioned models are either incorrect or incomplete. The wavelength dependence of the damage threshold in DKDP is consistent with defect assisted multiphoton absorption.

The experiments reported here use a constant focal spot geometry of 100 ± 5 μm, a temporal profile of 2.9 ± 0.1 ns, and polarization P:S extinction ratio of 1:1000. These parameters were maintained for wavelengths from 312 to 532 nm. The radiation source was an OPOTek Inc. ring cavity OPO (optical parametric oscillator) laser system. After passing through energy and polarization controlling elements, the output beam from the OPO was focused in the bulk of the sample. A combination of a HeNe laser and CCD camera, focused on the same volume as the OPO, was used to detect damage from the scatter signal.

Data were collected by irradiating up to 120 virgin (not previously exposed to high energy laser radiation) sites in the bulk of a single DKDP crystal with individual pulses at each wavelength. The percentage of sites with damage initiation was plotted vs fluence to generate a damage probability s curve (Fig. 1 inset). The energy was measured for each pulse and was combined with the average spot size to determine the fluence. The error for the laser fluence was determined by combining the 2% uncertainty in energy measurement and the standard deviation in the spot size, which varied with wavelength.

By extracting the 50% damage probability fluence for each of 21 s curves, a 50% damage probability vs wavelength graph is generated which demonstrates the overall wavelength dependence (Fig. 1). Figure 1 displays a number of striking features; most notable are the sharp steps in the damage threshold centered at 2.55 eV (487 nm) and 3.90 eV (318 nm). The region in between the steps exhibits

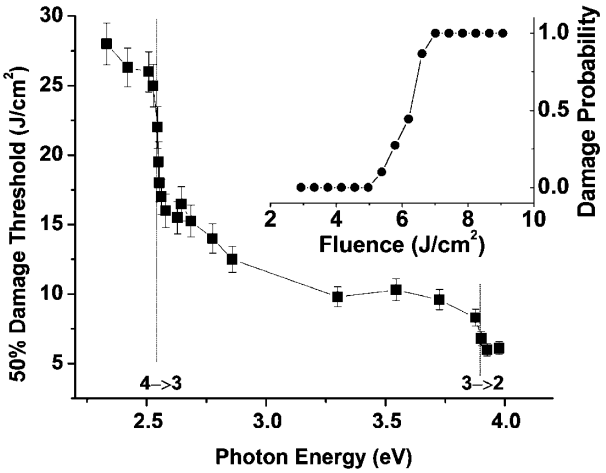

FIG. 1. A wavelength dependent damage threshold is obtained by plotting photon energy vs the fluence at which the sample damaged 50% of the time. The inset shows a damage probability s curve for 3.97 eV (312.4 nm).

a smooth decrease in the damage threshold with decreasing wavelength.

Replotting the s curve data in terms of photon energy at a constant fluence vs damage probability across each transition provides additional information regarding the nature of the transitions. In Fig. 2, the probability of damage at a fixed fluence is plotted vs photon energy. The damage probability for the transitions at 2.55 and 3.90 eV is plotted for 24 and 7.5 J/cm^2, respectively. When the midpoints of the transitions are overlapped (by subtracting 2.55 and 3.9 eV from the data surrounding the first and second steps, respectively), it becomes evident that both steps exhibit the same characteristics. The width of the transitions is established in Fig. 2 to be on the order of k_BT at room temperature.

To compare the energy at which the steps in the damage threshold occur, with respect to the DKDP band gap (ε_g),

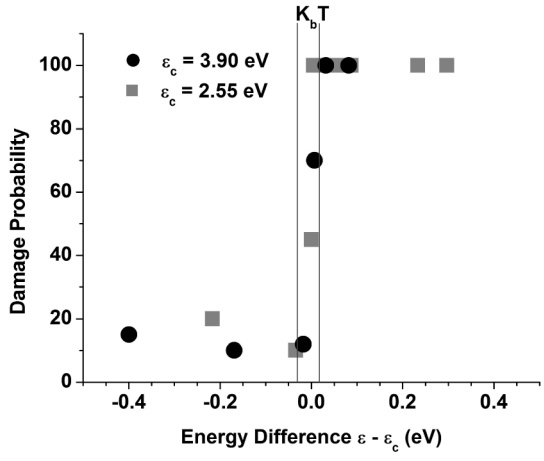

FIG. 2. Damage probability at fixed fluences plotted vs photon energy difference from each damage step ($\varepsilon_{\text{photon}} - \varepsilon_c$). The width of the transition is approximately k_BT.

it was first necessary to determine ε_g by UV transmission measurements. From the extinction of transmission, a lower bound to the band gap is determined to be $\boldsymbol{\varepsilon}_{gL} = 7.5$ eV. The band gap is generally identified by an absorption coefficient of 10^4 cm^{-1} [14]. As the absorption coefficient of our sample was only 100 cm^{-1} at 7.5 eV, the band gap is potentially as high as 9 eV [15]. The limiting factor in the UV absorption measurement was the thickness of the sample. Measurements made on KDP show a band gap to be between 8.0 and 8.8 eV [16]. Recent theoretical calculations suggest that the band gap of the two closely related materials should be similar if not identical [17].

The experimental results demonstrate the presence of sharp reductions in the damage probability at photon energies in the vicinity of fractions of an effective band gap ε_g/n, $n = 2, 3$. In addition, the width of both steps is very narrow ($\approx k_BT$) while the damage morphology indicates the presence of discrete initiation sites. The decrease in damage threshold across the steps is approximately from 27 to 16 J/cm^2 and from 9 to 6 J/cm^2, respectively.

By comparing these experimental features to the previously mentioned models for damage initiation, the relative contribution of each mechanism can be evaluated. Steps which occur at integer fractions of an energy (E_g) suggest multiphoton ionization; excitation of electrons to the conduction band by absorbing several photons simultaneously [3,18]. In a pure multiphoton ionization model, as the photon energy increases, the damage threshold would exhibit an abrupt drop as the number of photons needed to bridge the gap (the order) decreases by one, and the transitions will take place at photon energies of E_g/n. In wide gap materials, excitons are prominent at room temperature which could potentially lower the energy required to promote an electron to the conduction band by 1 eV or more [15]. For such a system, $E_g = (\boldsymbol{\varepsilon}_g - \Delta)$ and Δ is the binding energy associated with an exciton.

The steps observed in Fig. 1 (located at 2.55 and 3.9 eV) are both close to integer fractions of 7.8 eV, which is a likely location of the exciton peak in DKDP. The steps seen in Fig. 2 are close to 0.025 eV in width, which is much narrower than a typical width of a large band gap exciton peak. Therefore, the width of the steps in the damage threshold data is more likely governed by the thermal distribution of electrons in the valence band.

The expected change of the damage threshold across a step can be estimated from representative multiphoton cross sections ($\sigma^{(n)}$) for third, and fourth order absorption in wide band gap materials, which are on the order of 10^{-81} cm^6 s^2 and 10^{-114} cm^8 s^3, respectively [4,18,19]. The rate of energy absorption from a multiphoton process is given by [4,20]

$$\frac{d\varepsilon}{dt} = \frac{\varepsilon_g N}{(hc)^n}\sigma^{(n)}(I\lambda)^n, \tag{1}$$

where I is the laser intensity, n the absorption order, and ε_g the band gap. For multiphoton absorption in an ideal (defect-free) crystal, the active ion density (N) would be close to the atomic density. The electron density (N_e) necessary for rapid energy absorption would at most be the critical density (N_c) (where the plasma becomes opaque) but could be several orders of magnitude less, depending on the size of the plasma. Damage initiation sites from 3-ns laser pulses are generally on the order of $\sim$10 times the size of the incident wavelength. With an absorption length of 10λ, a minimum electron density of $0.01N_c$ is required for rapid energy absorption [21]. Since the critical electron density differs insignificantly over the width of the steps in the data of Fig. 2, approximately the same amount of energy must be first absorbed through the multiphoton mechanism on either side, making the exact value of the band gap unimportant. The intensity necessary for breakdown on each side of a step can be estimated by solving Eq. (1) for I_c:

$$I_c = \sqrt[n]{N_e/(N\sigma^{(n)}\Delta t)}hc/\lambda. \quad (2)$$

For the step at 487 nm, the critical density would be 5×10^{21} cm^{-3} [21]. The height of the step for a pure multiphoton mechanism may be estimated by computing the difference between the intensities necessary to produce N_c as the order of the multiphoton process changes. The predicted step at a change from 3 to 4 photon absorption is between 200 and 1500 J/cm^2 (for the lower and upper limits of N_e of $0.01N_c$ and N_c, respectively) rather than the observed value of 11 J/cm^2 at the 487 nm step.

The overall damage threshold for pure multiphoton absorption can be estimated as well. Using Eq. (2), for 355-nm radiation (three photon absorption) the N_c 10^{22} cm^{-3} suggests lower and upper bounds of $I_c = 3 \times 10^{10}$ W/cm^2 and 1.5×10^{11} W/cm^2, respectively. The observed damage threshold is $\sim 3 \times 10^9$ W/cm^2. For the 3-ns pulses used in this study, this corresponds to a predicted damage threshold ranging from 60 to 450 J/cm^2 compared to the observed value of 10 J/cm^2. For very small spot sizes (for which a pure multiphoton mechanism would be expected to dominate), damage thresholds in excess of 200 J/cm^2 have been reported [8,10]. The observed damage morphology is an additional indicator that pure multiphoton ionization is not the damage initiation mechanism [3]. Multiphoton damage is localized at the peak of a Gaussian beam, while we observe the presence of discrete initiation sites situated throughout the beam.

Before the pure multiphoton model can be dismissed, it is necessary to consider the possibility of field enhancement by small particles. Surface plasmon resonance in small (< 40 nm) particles has been shown to cause field enhancements of 2 orders of magnitude [22]. The field enhancement effect is sharply wavelength dependent and therefore would manifest itself as a narrow dip in the damage threshold for a single size of inclusion [23]. This model would require a uniform, continuous distribution of particle sizes to account for the wavelength dependence of the damage threshold similar to that observed in Fig. 1 by producing field enhancement at all wavelengths. However, particle size distributions are not, in general, uniform [24].

One of the first models which attempted to explain laser induced damage is the "lucky" electron avalanche breakdown model. This model suggests that some electrons are present in the conduction band before the laser pulse [5]. The free electrons oscillate in the lasers fields and liberate additional electrons by impact ionization. Electrons would multiply in this manner until opaque plasma is generated, facilitating rapid absorption during the remainder of the laser pulse. The damage threshold would increase at frequencies large compared to the inverse of the electron collision time, because of reduced coupling to the lattice. Contrary to the observed data, the avalanche model predicts no dependence of the damage threshold on the laser wavelength until the laser frequency approaches the inverse of the electron collision time [4].

A more recent model proposed that foreign particles included in the crystal lattice during growth act as gray bodies, absorbing a fraction of all incident radiation. The absorbed energy heats the surrounding host material causing a collapse of the band gap and plasma formation [7]. Because this gray particle model predicts laser damage will be initiated at the site of particles included during growth, it is reasonable to expect damage to occur at discrete localized centers, and not necessarily at the peak energy density of the laser. This is consistent with experimentally observed damage morphology in the 3 ns regime. However, for a uniform particle size distribution, the gray particle model predicts smooth $1/\lambda$ dependence for the damage threshold. This is roughly in agreement with the observed damage threshold data between the steps, but does not explain existence of the steps.

Extending the gray particle model by assuming two species of particles composed of materials with band gaps of 2.55 and 3.90 eV can provide a simple explanation that accounts for the steps in the damage threshold demonstrated in Fig. 1. Although this is a possibility, the presence of such a coupled set of impurities is not supported by optical spectroscopy, transmission data, or EPR spectroscopy [25,26].

In order to synthesize a model that accounts for lower than intrinsic damage threshold, the existence, size, and location of the steps, as well as the observed damage morphology, we propose a defect assisted multistep/photon mechanism. In this model, defect states in the gap alter the cross section for multiphoton absorption, in fact turning the process into a series of reduced order absorptions. In the presence of intraband defect states, excited state absorption can reduce the order of the

multiphoton process needed for an electron to make a transition to the conduction band. Whether the mechanism is a series of single photon absorptions or a mixture of single and multiphoton absorptions, this model accounts for the sharp steps in the damage threshold. The number of photons needed to create a free electron would be very sensitive to changes in photon energy near E_g/n. From this we would expect the next step ($n = 4$) in the damage threshold at or near 635 nm.

The phenomenological model proposed here assumes the existence of intraband states, and there is a reasonable expectation that these types of defects exist in DKDP. An example of a class of defects which has the properties needed are hydrogen vacancies, interstitial hydrogen atoms, or Frenkel pairs (an interstitial hydrogen near a vacancy). Such defects have recently been considered theoretically by Liu *et al.*, and can easily be included during growth or can result from impurity ion incorporation [17]. The band structure of these hydrogen defects has been calculated, and produces the states in the gap required by the proposed defect assisted multiphoton model [17].

Large band gap dielectric materials intentionally doped with impurity ions (such as laser crystals) offer the supporting evidence for the multistep defect assisted ionization process discussed above. Observation of emission from higher excited states of the impurity ions arising from excited state or two-photon absorption is common in these materials [27]. This process has been shown to be particularly efficient in some materials which led to the development of up-converted lasers where the laser wavelength is shorter to the pump wavelength [28]. Hot luminescence following excited state absorption has also indicated the population of transient vibronic states and electronic bottlenecks with varying lifetimes depending on the structure of the excited states [29]. Our model proposes that similar effects are taking place during exposure of defects in DKDP to high power laser irradiation. Depending on the laser wavelength, two or three photons absorbed by a number of neighboring defects can lead to a sufficient population of conduction band electrons to start the localized cascade electron multiplication process responsible for damage initiation.

Finally, the density of defects implied by this approach is considered. The overall damage thresholds are reduced because the effective cross section for a multistep process is larger than that of a single step. For example, the cross section of a three photon process is on the order of 10^{-81} cm^6 s^2 while the cross section for a combination of two-photon absorption followed by excited state absorption by a single photon is estimated to have an upper bound of 10^{-61} cm^6 s^2. Using this modified cross section in Eq. (2) with the observed damage threshold, a lower bound to the necessary defect density is estimated to be on the order of 10^7 cm^{-3}. Localized defect concentrations of this magnitude are reasonable in DKDP crystals, as demonstrated by the observation of fluorescing centers in the closely related crystal KDP which had a concentration on the order of 10^7 cm^{-3} [30]. As the fluorescing centers are believed to be comprised of multiple defects, their density is also a lower bound to the defect density.

The authors acknowledge suggestions provided by Mike Feit, Alexander Rubencheck, and Nick Kioussis, and assistance from Mike Staggs, Mike Runkel, Chance Carter, and Vladimir Liberman for performing the UV transmission measurements. This work was performed under the auspices of the U.S. Department of Energy by the University of California, Lawrence Livermore National Laboratory, under Contract No. W-7405-Eng-48.

[1] J. J. De Yoreo *et al.*, Int. Mater. Rev. **47**, 113 (2002).
[2] N. P. Zaitseva *et al.*, J. Cryst. Growth **180**, 255 (1997).
[3] B. C. Stuart *et al.*, Phys. Rev. B **53**, 1749 (1996).
[4] S. C. Jones *et al.*, Opt. Eng. **28**, 1039 (1989).
[5] N. Bloembergen, IEEE J. Quantum Electron. **10**, 375 (1974).
[6] Z. Qing *et al.*, Phys. Rev. B **65**, 024108 (2002).
[7] M. D. Feit *et al.*, Proc. SPIE Int. Soc. Opt. Eng. **2966**, 417 (1997).
[8] H. Yoshida *et al.*, Appl. Phys. B **70**, 195 (2000).
[9] F. Rainer *et al.*, Proc. SPIE Int. Soc. Opt. Eng. **1848**, 46 (1992).
[10] R. M. Oconnell, Appl. Opt. **31**, 4143 (1992).
[11] D. Du *et al.*, Appl. Phys. Lett. **64**, 3071 (1994).
[12] J. Natoli *et al.*, Proc. SPIE Int. Soc. Opt. Eng. **4932**, 224 (2002).
[13] J. Swain *et al.*, Appl. Phys. Lett. **40**, 350 (1982).
[14] E. D. Palik, *Handbook of Optical Constants of Solids* (Academic, Orlando, 1985).
[15] M. Fox, *Optical Properties of Solids* (Oxford University Press, Oxford, England, 2001).
[16] I. N. Ogorodnikov *et al.*, Opt. Spektrosk. **91**, 243 (2001).
[17] C. S. Liu *et al.*, Phys. Rev. Lett. **91**, 15505 (2003).
[18] V. Nathan *et al.*, J. Opt. Soc. Am. B **2**, 294 (1985).
[19] C. Gorling *et al.*, Appl. Phys. B **74**, 259 (2002).
[20] A. Schmid *et al.*, Phys. Rev. B **16**, 4569 (1977).
[21] F. F. Chen, *Introduction to Plasma Physics and Controlled Fusion* (Plenum, New York, 1984).
[22] J. P. Kottmann *et al.*, Appl. Phys. B **73**, 299 (2001).
[23] K. Kneipp *et al.*, Chem. Rev. **99**, 2957 (1999).
[24] D. Risovic, Appl. Opt. **41**, 7092 (2002).
[25] S. G. Demos *et al.*, J. Appl. Phys. **85**, 3988 (1999).
[26] N. Y. Garces *et al.*, J. Appl. Phys. **89**, 47 (2001).
[27] H. L. Xu *et al.*, Phys. Rev. B **66**, 035103 (2002).
[28] A. J. Silversmith *et al.*, Appl. Phys. Lett. **51**, 1977 (1987).
[29] S. G. Demos *et al.*, Opt. Lett. **18**, 522 (1993).
[30] S. G. Demos *et al.*, Opt. Lett. **26**, 1975 (2001).